Computational models of human response to urban heat

From physiology to behaviour

Melnikov, V.

Publication date
2021

Chapter 2

System dynamics of human body thermal regulation in outdoor environments

Thermal regulation serves a need of human body to maintain the stable core temperature to ensure the proper functioning of all the biological systems. Heat exchange between the human body and the environment is regulated by the physiological thermoregulatory system, which is the first line of response to thermal stimulation. It is the thermophysiological state, determined by both the environment and the system of thermal regulation, which drives the human response on other levels considered in this thesis, which in turn are employed to bring this state as close as possible to a neutral one. Understanding and being able to accurately reproduce the physiological response is central to the study of response on other levels. This chapter covers the system dynamics model of human body thermal regulation, which along with providing the model of human response on the physiological level also serves as a supporting model for the studies in the next chapters.

Abstract

Thermal comfort of people in outdoor urban spaces is a growing concern in cities due to climate change and urbanisation. In outdoor settings the climate

This chapter is based on Melnikov, V., Krzhizhanovskaya, V. V., Lees, M. H., & Sloot, P. M. A. (2018). System dynamics of human body thermal regulation in outdoor environments. *Building and Environment, 143*, 760-769.

and behaviour of people are more dynamic than in indoor situations, therefore a steady state of the thermoregulatory system is rarely reached. Understanding the dynamics of outdoor thermal comfort requires accurate predictive models. In this chapter we extend a classical two-node model of human body thermal regulation. We give a detailed description and interpretation of all the components and parameter values and test the dynamics of the model against experimental data. We propose a modification of the skin blood flow model which, while keeping realistic values and responsiveness, improves skin temperature prediction nearly fourfold. We further analyse the sensitivity of the model with respect to climatic and personal parameters. This analysis reveals the relative importance of, for instance, air temperature, wind speed and clothing, in thermoregulatory processes of the human body in various climatic settings. We conclude, that our model realistically reproduces the dynamics of aggregate measures of human body thermal regulation. Validated for cool, warm and hot environments, the model is shown to be accurate in terms of its dynamics and it is conceptually and computationally far more efficient than any existing multi-node and multi-part model.

2.1 Introduction

Thermal comfort of people in outdoor urban spaces is a growing issue for many of the world's cities due to the global processes of climate change and urbanisation. Heat is not only related to physiological and psychological stress, but also to population morbidity and mortality [94]. The physiological thermal regulation system is one of the key means of adaptation of human beings to heat in outdoor environments. The state of this system, typically described with parameters such as core-, skin- temperature or sweating rate, defines stress and to a large extent determines an individual's level of comfort. In outdoor environments, due to the large variability of the outdoor climate, and people's activity in urban settings, the thermoregulatory system is highly dynamic. To model outdoor thermal comfort (OTC) of people, one should be able to accurately reproduce individual dynamics of the thermoregulatory system. Such OTC models could be applied to understand

how to design urban environments and maximise the comfort of individuals. For example, how to design spaces that reduce radiance, increase airflow or promote heat reduction due to evapotranspiration. Ideally these models should be applied to whole populations of individuals in order to understand how an environment impacts those individuals. It is therefore important to minimise the complexity of the model while retaining accurate dynamics.

Multiple models have been proposed to predict the state of human body thermal regulation. Probably the most influential is the 25-node model proposed by Stolwijk [95, 96], consisting of one central blood "node" and 24 body "nodes" (six body segments, each with four compartments). Several improvements have been introduced to the model since then, in order to better predict the dynamics of local response of body parts, for instance increasing the number of body compartments and body parts [97, 98, 99]. A model that simplified the original model for prediction of the overall thermophysiological state was proposed by Gagge in 1972 [100]. Gagge's model has since been used intensively in studies of thermal comfort. It was adopted by the ASHRAE standard for indoor thermal environments [101] and used to define the Physiologically Equivalent Temperature (PET) [71], which is the most commonly used thermal comfort index. Properties of both Stolwijk's and Gagge's model were analysed for steady state values predictability in indoor environments [96, 102]. These studies however were lacking evaluation of the dynamic behaviour. Munir et al. [103] reevaluated the model of Stolwijk in terms of its dynamical properties and analysed several adjustments to the model, the authors demonstrated that the dynamics can closely reproduce empirical data. Based on this data Foda et al. [104] evaluated three other models: multi-node multi-part Fiala's model [97], the UCB model [99] and a two-node multi-part MS-Pierce model [105]. The results demonstrate significant discrepancy in the dynamics of the models. The authors of the study do not propose a measure for quantitative evaluation of the model's accuracy in terms of its dynamic behaviour. Gagge's two-node model has been used to model the dynamics of thermal regulation of pedestrians in outdoor environments [106, 107], but has not been extensively analysed for its dynamical properties. A comprehensive review of existing models, their evaluation and application can be found in [108].

The absence of analysis of the simplified two-node model, as well as weak results of dynamic performance of the other, much more sophisticated, models suggest the evaluation and reconsideration of the two-node model. In this study we implement the classical two-node model of Gagge based on descriptions found in [102, 109, 105]. We rethink the representation of the model by applying concepts from system dynamics: namely stock-and-flow diagrams. System dynamics uses energy stocks and flows to define the dynamics of the system and the causal relationships between parameters. We then analyse the performance of the model in a dynamic environment and use root mean square error for its quantitative evaluation. We demonstrate how the system dynamics approach can help to identify parameters responsible for the poor dynamics and show significantly improved model dynamics by parameter calibration against Munir's data [103]. We demonstrate the validation of the model for cool, warm and hot environments. Global sensitivity analysis adds another dimension to the model, allowing for the identification of the most important environmental and individual parameters in different climates.

The remainder of this chapter is organised as follows: we provide a system dynamics representation of the model in Section 2.2 and its exhaustive formulation in Section 2.3. We then investigate the performance of the model and report results of model calibration and sensitivity analysis in Section 2.4. We discuss the results in Section 2.5 and conclude the chapter with Section 2.6.

2.2 System dynamics representation of the model

Two nodes of the model of Gagge [100], core and skin, are represented in our system dynamics model as two stocks storing the energy within the body, where the energy is translated into temperatures of two nodes: T_{core} and T_{skin}, see Figure 2.1.

Flows of the model represent energy fluxes within, to and from the human body: metabolic rate M, generation of heat through shivering Sh, heating and humidification of inhaled air Re, mechanical work rate W, core-skin heat transfer CS, convection C, latent heat flux through evaporation of sweat E

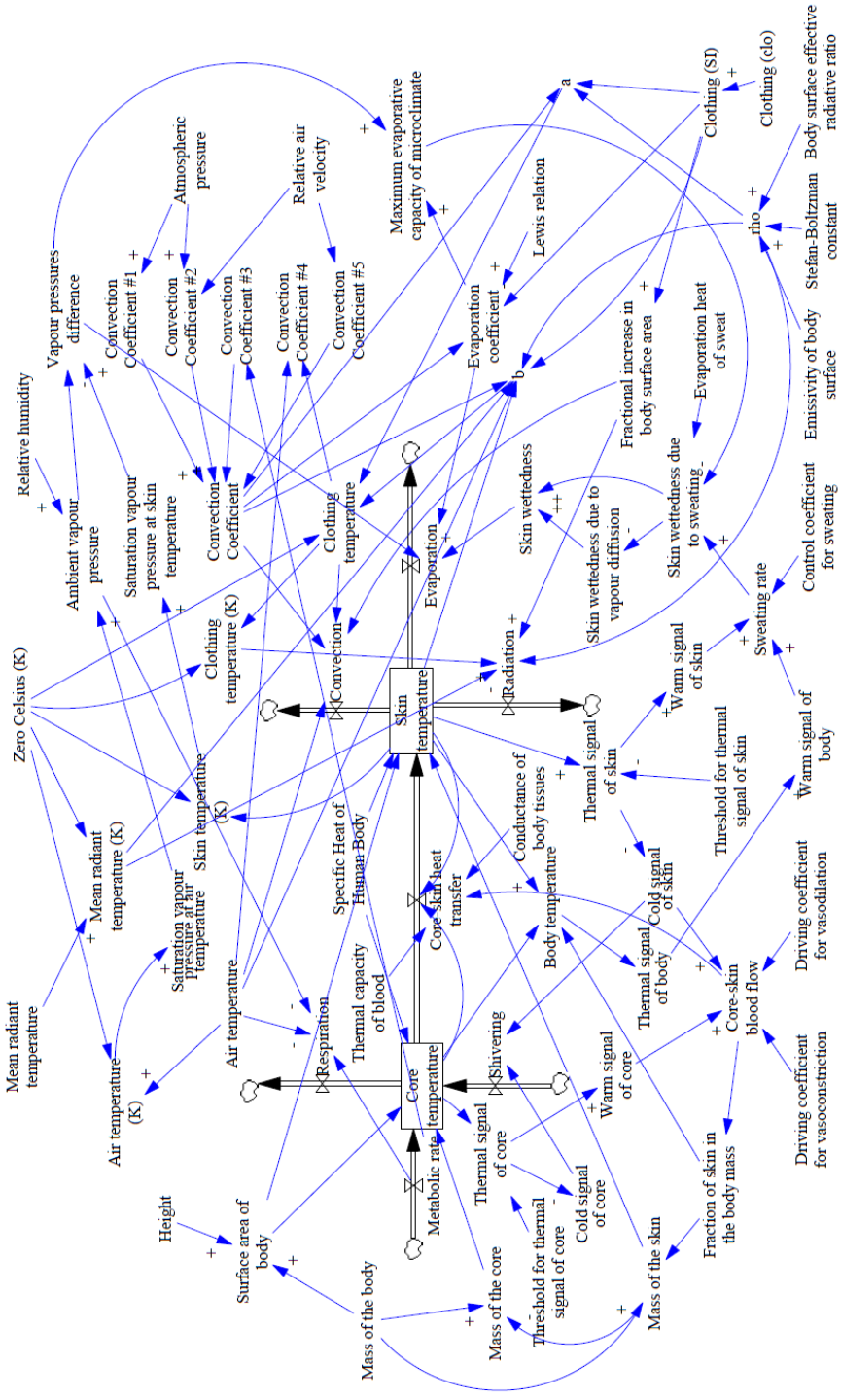

FIGURE 2.1: Stock-and-flow diagram of a two-node model of the thermoregulatory system. Rectangles with solid stroke represent two energy stocks: core and skin, black-headed arrows are energy flows within, to and from the human body, blue arrows represent causal relationships between parameters of the model

and radiative heat exchange R (note that all the fluxes are defined with respect to the unit of body surface area).

Heat storage rate St is then defined as the sum of all fluxes coming to and from the body, corresponding to cooling of the body when negative and to heating when positive:

$$St = M + Sh - Re - W - C - E - R \quad \left[\frac{W}{m^2}\right] \tag{2.1}$$

The steady state of the system is then defined as the state where energy balance is found, thus $St = 0$. The dynamics of the system is always moving towards steady state and individial and microclimate parameters determine whether and when the system will converge to this state.

Figure 2.1 shows the stocks-and-flows diagram traditionally used in system dynamics modelling. It depicts the two cores as rectangles with solid stroke connected between each other and thermal environment through flows – fluxes as described above, shown as arrows with 'valves'. Arrows identify causal relationships between the parameters, variables, stocks and flows of the model, with polarity signs on their heads revealing the influence of their change in the dependent variable, assuming other determining parameters are fixed.

We further define all the fluxes through the parameters of the model and then give the final equations of the nodes dynamics expressed as fluxes.

2.3 Formulation of the model

2.3.1 Parameters of the model

We define the constants used in the derivation below by the values indicated in the first section of Table 2.1.

The model considers the individual parameters of a person listed in the second section of Table 2.1. Many variables of the model are defined with respect to surface area of human body, which is estimated by Dubois formula

TABLE 2.1: Parameters of the model

Param.	Value	Units	Range	Description	Ref.
			Constants		
σ	$5.67 \cdot 10^{-8}$	$\frac{W}{m^2 \cdot K^4}$	–	Stefan-Boltzmann constant	–
c_b	3492	$\frac{J}{kg \cdot K}$	–	Specific heat of human body	[102, 109]
c_{bl}	1.163	$\frac{W \cdot hr}{l \cdot K}$	–	Thermal capacity of blood	[102, 109]
c_{sw}	2426	$\frac{J}{gr}$	–	Evaporation heat of sweat	[110]
k_b	5.28	$\frac{W}{m^2}$	–	Conductance of body tissues	[102, 109]
			Individual parameters		
m_{body}	75.0	kg	–	Weight	–
h_{body}	1.8	m	–	Height	–
M	80	$\frac{W}{m^2}$	–	Metabolic rate	[101]
μ_W	[0;1]	–	–	Mechanical work efficiency	[111, 112, 113]
I_{cl}	0.155	$\frac{K \cdot m^2}{W}$	–	Clothing level	[101]
			Climatic parameters		
T_{air}	–	$^\circ C$	–	Air temperature	–
T_{mrt}	–	$^\circ C$	–	Mean radiant temp.	[114]
v	–	$m \cdot s^{-1}$	–	Rel. air speed	–
p_a	–	$mmHg$	–	Atmospheric pressure	–
RH	–	$\%$	–	Relative humidity	–
			Static parameters		
T^*_{body}	36.49	$^\circ C$	–	Neutral temp. of the body	[102, 109]
T^*_{core}	36.8	$^\circ C$	36.6–36.8	Neutral temp. of the core	[109]
T^*_{skin}	33.7	$^\circ C$	33.7–34.0	Neutral temp. of the skin	[109]
q^*_{bl}	6.3	$\frac{l}{hr \cdot m^2}$	–	Neutral skin blood flow	[100]
α_{rad}	0.72	–	0.61–0.79	Ratio of effective radiative area	[115]
c_{con}	0.5	$^\circ C^{-1}$	0.1–0.5	Coef. for vasoconstriction	[109]
c_{dil}	200	$\frac{l}{hr \cdot m^{2,\circ} C}$	50–240	Coef. for vasodilation	[109]
c_{rsw}	170	$\frac{gr}{m^{2,\circ} C \cdot hr}$	$\pm 50\%$	Coef. for sweating rate	[102]
c_{shiv}	19.4	$\frac{W}{m^{2,\circ} C^2}$	–	Coef. for shivering	[102, 109]
ϵ_{cl}	0.97	–	0.92–1.0	Emissivity of clothed body	[102, 109]

[116]:

$$A_{Du} = 0.203 \cdot m_{body}^{0.425} h_{body}^{0.725} \qquad \left[m^2\right] \tag{2.2}$$

The level of clothing of a person determines the increase in body surface area reported in [105] as follows:

$$f_{cl} = \begin{cases} 1 + 1.290 \cdot I_{cl} & \text{if} \quad I_{cl} < 0.072, \\ 1.05 + 0.645 \cdot I_{cl} & \text{otherwise.} \end{cases} \tag{2.3}$$

Clothed body surface area then can be calculated as follows:

$$A_{cl} = f_{cl} \cdot A_{Du} \qquad \left[m^2\right] \tag{2.4}$$

The microclimate parameters considered in the model are listed in the third section of the Table 2.1. Other important parameters are derived from these values. Saturation vapour pressure is estimated according to [102]:

$$p_{sat} = \exp\left(18.67 - \frac{4030.18}{T_{air} + 235}\right) \qquad [mmHg] \tag{2.5}$$

From which the ambient vapour pressure is derived:

$$p_{va} = p_{sat} \frac{RH}{100} \qquad [mmHg] \tag{2.6}$$

Certain parameters of the model are usually set to a fixed value, however different authors have estimated different values for the parameters and in some cases parameters vary between individuals. The last section of the Table 2.1 lists these parameters. Conventional values of these parameters and a range of possible values are shown where appropriate.

2.3.2 Model variables

Thermal signals

There are three thermal signals, which are regulating the system, derived from temperatures of core, skin and the whole body.

$$S_{core} = T_{core} - T^*_{core} \qquad [^\circ C]\,, \tag{2.7}$$

$$S_{skin} = T_{skin} - T^*_{skin} \qquad [^\circ C]\,, \tag{2.8}$$

$$S_{body} = T_{body} - T^*_{body} \qquad [^\circ C]\,. \tag{2.9}$$

Where T_{body} is the average weighted body temperature as defined in eq. 2.20. The signal of the whole body S_{body} is regulating the sweating response. The respective cold and warm signals are defined as follow:

$$S^+_{core} = max(0,\ S_{core}) \qquad [^\circ C]\,, \tag{2.10}$$

$$S^-_{core} = min(S_{core},\ 0) \qquad [^\circ C]\,, \tag{2.11}$$

$$S^+_{skin} = max(0,\ S_{skin}) \qquad [^\circ C]\,, \tag{2.12}$$

$$S^-_{skin} = min(S_{skin},\ 0) \qquad [^\circ C]\,, \tag{2.13}$$

$$S^+_{body} = max(0,\ S_{body}) \qquad [^\circ C]\,, \tag{2.14}$$

$$S^-_{body} = min(S_{body},\ 0) \qquad [^\circ C]\,. \tag{2.15}$$

Blood flow regulation

Thermal signals of core and skin define the blood flow thermal regulation through vasoconstriction and vasodilation. The warm signal of the core being multiplied with the coefficient of vasodilation increases the blood flow from core to skin, whereas the cold signal of the skin, multiplied with coefficient of vasoconstriction, reduces it. For core-to-skin blood flow this relationship is:

$$q_{bl} = \frac{q^*_{bl} + c_{dil} \cdot S^+_{core}}{1 - c_{con} \cdot S^-_{skin}} \qquad \left[\frac{l}{hr \cdot m^2}\right] \tag{2.16}$$

Masses of nodes

Blood flow regulation determines how much blood is exchanged between the nodes, implying that the boundary between nodes moves with changes in the blood flow between the nodes. The higher this blood flow – the less the fraction of the skin compartment in the total mass of the body. The fraction of skin in the body mass is then defined as follows:

$$\alpha_{skin} = 0.0418 + \frac{0.7425\,[l/(hr \cdot m^2)]}{q_{bl} + 0.5854\,[l/(hr \cdot m^2)]} \tag{2.17}$$

Then the masses of the skin and core compartments are:

$$m_{skin} = \alpha_{skin} \cdot m_{body} \qquad [kg]\,, \tag{2.18}$$

$$m_{core} = m_{body} - m_{skin} \qquad [kg]\,. \tag{2.19}$$

And the average weighted body temperature:

$$T_{body} = \alpha_{skin} \cdot T_{skin} + (1 - \alpha_{skin}) \cdot T_{core} \qquad [^{\circ}C] \tag{2.20}$$

2.3.3 Flows

Flows to and from the core

The metabolic rate M represents the internal heat production due to food digestion. This rate is highly dependent on the type of activity performed by an individual and it is usually estimated through reference tables, for example in Table 2.1 the value for M is given for sedentary light office work activity.

The rate of mechanical work W represents the amount of energy spent to perform some physical activity (i.e. not for heating the body). For sitting in the office, it is usually assumed to be zero. For walking, these values are calculated through the mechanical work efficiency μ_W (see eq. 2.21), which is maximised at the optimal walking speed of approximately 1.2 m/s. $\mu_W \in [0.21; 0.23]$ if defined relative to the total metabolic rate [111]. Some authors define this efficiency relative to the total minus standing or basal metabolic rate, which results in a higher estimated value of μ_W [112, 113]. In case of running, unlike for walking, the efficiency grows with increasing

speed, reaching the value of $\mu_W = 0.8$. This is due to the difference in physics of the two types of activity.

$$W = \mu_W \cdot M \qquad \left[\frac{W}{m^2}\right] \tag{2.21}$$

Having cold signals from both core and skin nodes implies that the additional heat is produced by the body through shivering, defined as follows [102, 109]:

$$Sh = c_{shiv} \cdot S^-_{core} \cdot S^-_{skin} \qquad \left[\frac{W}{m^2}\right] \tag{2.22}$$

The inhaled air is humidified and heated within the respiratory system, which results in energy expenditure. The amount of inhaled air is proportional to the metabolic rate. Respiration heat flux is then estimated by:

$$Re = \frac{M}{10^4} \cdot [\underbrace{14 \cdot (34 - T_{air})}_{\text{heating}} + \underbrace{23 \cdot (44 - p_{va})}_{\text{humidification}}] \left[\frac{W}{m^2}\right], \tag{2.23}$$

where p_{va} is ambient vapour pressure defined by eq. 2.6.

Core-to-skin heat transfer

The core exchanges heat with the outer compartment of the body – skin. This exchange depends on the difference in temperature of these nodes and blood flow between them:

$$CS = (k_b + c_b \cdot q_{bl})(T_{core} - T_{skin}) \qquad \left[\frac{W}{m^2}\right] \tag{2.24}$$

Flows to and from the skin

Being an outer compartment of the body, the skin is the major source of energy exchange between the body and its environment. This energy exchange happens through three major fluxes: convection, evaporation and radiation. Conduction is usually considered not significant in the range of models that we consider.

Convection is highly dependent on the airflow speed and for different environments different coefficients for convection are estimated:

$$h_{c1} = 3\left(\frac{p_a}{760}\right)^{0.53} \quad \left[\frac{W}{m^{2\circ}C}\right], \tag{2.25}$$

$$h_{c2} = 8.6\left(v \cdot \frac{p_a}{760}\right)^{0.53} \quad \left[\frac{W}{m^{2\circ}C}\right], \tag{2.26}$$

$$h_{c3} = 5.66\left(\frac{M}{58.2} - 0.85\right)^{0.39} \quad \left[\frac{W}{m^{2\circ}C}\right], \tag{2.27}$$

$$h_{c4} = 2.38(T_{clo} - T_{air})^{0.25} \quad \left[\frac{W}{m^{2\circ}C}\right], \tag{2.28}$$

$$h_{c5} = 12.1\sqrt{v} \quad \left[\frac{W}{m^{2\circ}C}\right]. \tag{2.29}$$

Where T_{clo} is the clothing temperature defined in eq. 2.34. The largest h_c value is used to estimate the convective flux:

$$h_c = \max(h_{c1}, h_{c2}, h_{c3}, h_{c4}, h_{c5}) \quad \left[\frac{W}{m^{2\circ}C}\right] \tag{2.30}$$

Finally the convective flux is defined as follows:

$$C = h_c \cdot f_{cl} \cdot (T_{clo} - T_{air}) \quad \left[\frac{W}{m^2}\right] \tag{2.31}$$

Radiative heat exchange between human body and environment is mainly determined by the difference in clothing temperature and mean radiant temperature.

$$R = f_{cl} \cdot \alpha_{rad} \cdot \epsilon_{cl} \cdot \sigma \cdot (T^4_{clo.K} - T^4_{MRT.K}) \quad \left[\frac{W}{m^2}\right] \tag{2.32}$$

where $T_{clo.K}$ and $T_{MRT.K}$ are clothing and mean radiant temperature in Kelvin.

Once the expressions for C and R are introduced, the clothing temperature can be found as the one under which the heat transfer from skin through clothing on the surface of the clothes is equal to the sum of convective and radiative heat exchange between clothing and environment:

$$(T_{clo} - T_{skin})/I_{cl} = C + R \quad \left[\frac{W}{m^2}\right] \tag{2.33}$$

The C and R terms can be substituted into the equation to allow it to be solved for T_{clo} in closed form, however in practice the value is easier to find computationally using numerical optimisation:

$$T_{clo} = \underset{T_{clo}}{\arg\min} \left(|(T_{clo} - T_{skin})/I_{cl} - C - R| \right) \ [^{\circ}C] \tag{2.34}$$

Latent heat removal through evaporation of sweat on the skin surface depends on the convection potential of the environment and clothing level, which is reflected in the coefficient for evaporation:

$$h_e = \frac{L \cdot h_c}{1 + 0.92 \cdot I_{cl} \cdot h_c} \quad \left[\frac{W}{m^2 \cdot mmHg} \right] \tag{2.35}$$

Where L is the Lewis' relation and is set to $L = 2.2$ for sea level altitude.

The sweating rate is determined by the body and core warm signal:

$$r_{sw} = \frac{c_{rsw}}{3600} \cdot S^{+}_{body} \exp\left(\frac{S^{+}_{skin}}{10.7} \right) \quad \left[\frac{gramm}{m^2 \cdot s} \right] \tag{2.36}$$

The difference between saturation vapour pressure p_{clo} at clothing temperature T_{clo} (calculated similar to eq. 2.5) and ambient vapour pressure, determine the maximum evaporative capacity of the environment (assuming skin wettedness $w_{skin} = 1$):

$$p_{diff} = p_{clo} - p_{va} \quad [mmHg], \tag{2.37}$$

$$E_{max} = 1 \cdot h_e \cdot p_{diff} \quad \left[\frac{W}{m^2} \right]. \tag{2.38}$$

Skin wettedness level due to sweating:

$$w_{sw} = \min\left(\frac{r_{sw} \cdot c_{sw}}{E_{max}}, 1 \right) \tag{2.39}$$

Wettedness of the skin due to sweating is $w_{sw} \in [0; 1]$, excessive sweat which cannot be evaporated is dripping. Natural wetteness of the skin due to the

vapour diffusion through it and total skin wettedness are then defined as:

$$w_{dif} = 0.06 \cdot (1 - w_{sw}), \tag{2.40}$$

$$w_{sk} = w_{dif} + w_{sw}. \tag{2.41}$$

Finally, the expression for the evaporative heat flux is:

$$E = w_{sk} \cdot h_e \cdot p_{diff} \quad \left[\frac{W}{m^2}\right] \tag{2.42}$$

Governing equations for system dynamics of thermal regulation

After the flows are calculated for the model at time t seconds the value of stocks at time $t + \Delta t$ are calculated as follows:

$$T_{core}(t + \Delta t) = T_{core}(t) + \frac{A_{Du}[M - W - Re - CS]}{c_b \cdot m_{core}} \Delta t, \tag{2.43}$$

$$T_{skin}(t + \Delta t) = T_{skin}(t) + \frac{A_{Du}[CS - C - E - R]}{c_b \cdot m_{skin}} \Delta t. \tag{2.44}$$

2.4 Model analysis and results

2.4.1 Initial validation

For validation of the model's static and dynamic performance we simulated the dynamics of skin and core temperatures for the experimental schedule reported in Munir et al. [103]. In the experiment subjects were moving between climatic chambers with different microclimates according to a neutral-cool-neutral-warm-neutral schedule (see Figure 2.2 for duration and climate parameters of stages of the schedule).

The model was initialised with climatic parameters from the first scenario and average personal characteristics (height, weight and clothing) and simulated with one-second time steps, for which model has shown numerical stability.

As can be seen from Figure 2.2, the general dynamics and absolute values of the skin and core temperatures are well captured by the model. However,

the growth of skin temperature at the third stage of the schedule is significantly slower than the growth observed in the experiments. While this is acceptable behaviour for a model of thermoregulation in static indoor thermal environments, for modeling dynamic thermal sensation in transient outdoor environments this can become a reason for inaccurate estimation of people's physiological state and their overall thermal sensation. Further in this chapter we are focusing on the dynamics of skin temperature, as it is In the next section we show how the system dynamics approach helps to identify the component of the model responsible for these inaccurate dynamics and demonstrate how parameter tuning can improve the model's dynamics.

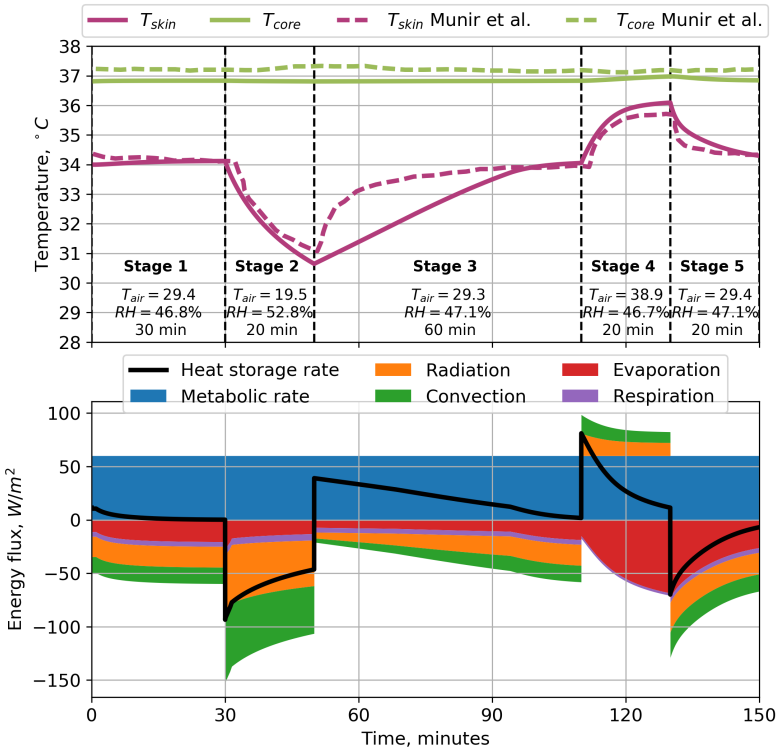

FIGURE 2.2: Comparison of the system dynamics simulation results with empirical data [103] (top) and simulated energy fluxes of heat exchange with the environment (below), where positive flux has heating effect on body and negative flux has cooling effect.

2.4.2 Model calibration

The difference in dynamics of the skin temperature between experimental data and simulation suggests that the skin temperature is not changing fast enough for certain physiological states and varying environmental conditions (third stage in Figure 2.2). To investigate the factors that influence skin temperature dynamics, we construct a causal tree for the skin temperature node stock-and-flow diagram (see Figure 2.3).

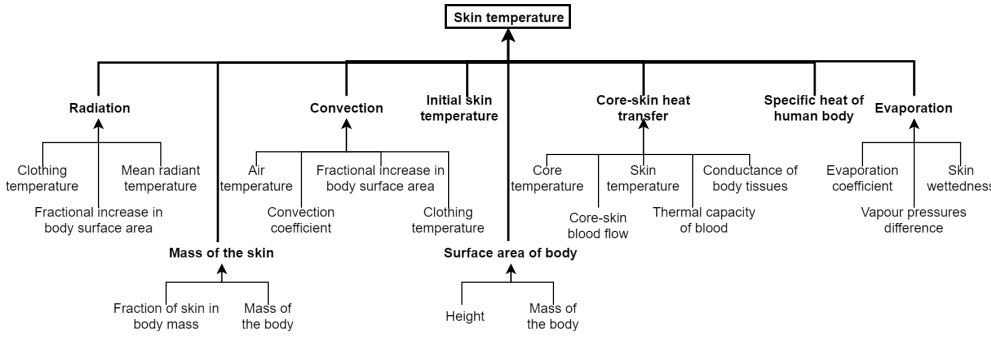

FIGURE 2.3: Causal tree of skin temperature of depth 3.

We find that parameters influencing skin temperature are radiation, convection, evaporation flows and core-skin heat transfer. The first three flows, however, do not have a sufficient gradient between the skin temperature and the environment to transfer heat from the environment to the body. The only source of heat significantly influencing the heating process is the core-skin heat transfer. This term depends on multiple parameters, only one of which is available for adjustment: core-skin blood flow. Other parameters are either constants or have valid values according to observations (core and skin temperature before the change in the microclimate conditions). The equation for core-skin blood flow is estimated in the original model from empirical data, that is, it is based on data, but not on the underlying physical process. The parameters influencing it are c_{con}, c_{dil}, T^*_{core}, T^*_{skin}, which can be chosen arbitrarily from the ranges mentioned in Table 2.1. We ran global optimisation procedures for these parameters minimizing the difference between experimental and simulated dynamics of skin temperature, where the difference is expressed in terms of root mean square error (RMSE).

Table 2.2 lists three sets of parameters for which model was simulated. The first parameter set represents the most commonly used in literature; the second is the result of parameters optimisation procedure, where parameters were allowed to vary within the ranges found in literature and listed in Table 2.1. The third set of parameters is a result of optimisation procedure, where we allow tuning of the neutral core-skin blood flow q^*_{bl} (with a reported value of $q^*_{bl} = 6.3\ l \cdot hr^{-1} \cdot m^{-2}$ [102, 109]). We allow q^*_{bl} to vary within the range of [4;12] $l \cdot hr^{-1} \cdot m^{-2}$ (established experimentally after several runs of optimisation procedure), taking into account that all the other parameters also have wide ranges reported in literature [102, 109]. The results are shown in Figure 2.4a, where the curve number represents the simulated dynamics of T_{skin} using the corresponding set of core-skin blood flow parameters listed in Table 2.2, i.e. T_{skin1} corresponds to skin temperature dynamics in model with original set of parameters. We can conclude that tuning parameters within reported ranges does not give a significant improvement of skin dynamics T_{skin2}. The tuned value of $q^*_{bl} = 10.7\ l \cdot hr^{-1} \cdot m^{-2}$ *does* significantly improve the dynamics of skin temperature T_{skin3}, resulting in a nearly four-fold reduction in RMSE.

Adjustment of q^*_{bl} requires the validation of the resulting q_{bl} against the values generated with the conventional set of parameters. Figure 2.4b shows the dynamics of q_{bl} for each of the parameter sets from Table 2.2. Comparing the values of the core-skin blood flow obtained by the calibrated models (q_{bl2} and q_{bl3}) to the model with the original set of parameters (q_{bl1}), we expect that:

1. the flow values during the neutral stage (stage 1) to be close to those of q_{bl1};

2. a reduced response to cooling stage 2: a too big drop in q_{bl} during this stage would lead to the inability of T_{skin} to restore fast enough during the subsequent stage;

3. a reduced response to the warming stage 4, since it is unrealistically high and leads to overestimation of T_{skin}.

From Figure 2.4b it follows that q_{bl3} meets all the listed expectations. Therefore, from here on wards we will use set 3 in our simulations, this will result

in significantly improved dynamics of T_{skin}.

Set no.	q^*_{bl}	T^*_{core}	T^*_{skin}	c_{dil}	c_{con}	T_{skin} RMSE, $°C$
1	6.3	36.8	33.7	200	0.5	0.665
2	6.3	36.6	33.7	50	0.1	0.549
3	10.7	36.7	33.7	50	0.1	0.182

TABLE 2.2: Model parameters used in simulations shown in Figure 2.4a

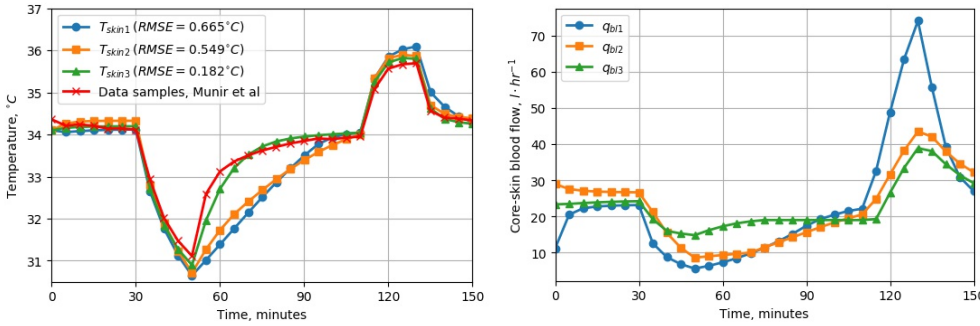

(A) Skin temperature T_{skin}

(B) Skin blood flow q_{bl}

FIGURE 2.4: The dynamics of skin temperature and skin blood flow for Munir's schedule simulated for three sets of parameters of skin blood flow (see Table 2.2) compared to empirical data.

2.4.3 Performance of the calibrated model

We compared the results of our calibrated model with other models reported in the literature for the first schedule of Munir et al. The data for other models was obtained through digitisation of plots from the original sources: Stolwijk's (multi-node, multi-segment) model [103], Fiala's (multi-node multi-segment) model and MS-Pierce (two-node, multi-segment) model [104]. The performance of the models was evaluated with measure of RMSE. Figure 2.5 demonstrates the dynamics of the existing models and the current model compared with empirical data. The dynamics of the current model is significantly

better than Fiala's model and MS-Pierce's model and is more or less equivalent to Stolwijk's multi-node multi-segment model in terms of RMSE. In summary we can conclude that the tuned model outperforms some of the existing, more sophisticated models, and performs similarly to Stolwijk's more complex model.

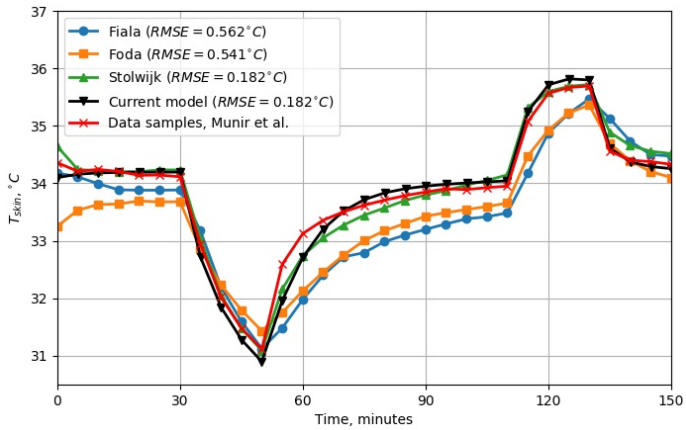

FIGURE 2.5: The comparison of current model with the dynamics of other found in literature.

Munir et al. also reported the second schedule with prolonged stages 2, 4 and 5. We simulated original model of Gagge's and our model for this scenario and compared it with the experimental data and Stolwijk's model simulation reported by Munir et al [103]. The results are provided in Figure 2.6 and demonstrate good consistency of the model, especially when compared with the original one.

2.4.4 Sensitivity analysis

Sensitivity analysis allows for understanding the sensitivity of the model's output to variations in the model's inputs. Performing the analysis helps to uncover the relative influence of parameters on the model's output. Knowing which parameters the model is sensitive or insensitive to can help to identify which parameter must be estimated more accurately through data or experimentation. We performed variance-based global sensitivity analysis [117] of the model for 8 parameters: 4 climatic parameters (T_{air}, T_{MRT}, RH and v),

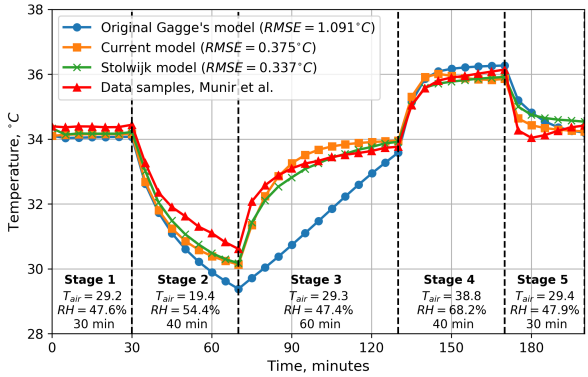

FIGURE 2.6: The comparison of current model with the dynamics of Gagge's original model, Stolwijk's model and empirical data from second scenario of Munir et al. [103].

and 4 individual parameters (M, I_{cl}, m_{body} and h_{body})[1]. Sensitivity analysis of the model was performed for two sets of parameters, representing a moderate summer climate (e.g. Europe or North America) and a hot and humid climate representing hot and humid (sub-) tropical climates (e.g. Singapore or Thailand). The ranges of parameters were chosen within reasonable values and are not intended to set strict definition of these climates. For each type of climate the parameters of the model were sampled from the space defined by the respective ranges using Saltelli extension of Sobol's sequence [119], with total number of parameter samples $N = 1800$ ensuring sufficient and uniform coverage of the sample space. We analysed the sensitivity of the model in terms of the temperatures of two compartments: core and skin.

The results shown in Figure 2.7 demonstrate that the sensitivity of the parameters is different for the two different climates. In the moderate climate the skin temperature is shown to be most sensitive to the level of clothing followed by air temperature. Interestingly, in hot and humid climates the sensitivity of these parameters flip: air temperature becomes more sensitive parameter than clothing level. The third most important parameter for skin temperature in both climates is wind speed. For core temperature sensitivity in moderate climates, metabolic rate is the most important parameter, followed by wind speed and air temperature. In hot and humid climate sensitivity to

[1]Using the Python library SALib 1.1.0 [118]

these parameters is in the following order: air temperature, wind speed and metabolic rate. This analysis allows to identify the most critical parameters influencing thermal regulation in different climates. For example, in Singapore, a country with hot and humid climate, the most critical factors affecting skin temperature dynamics are air temperature, clothing insulation and wind speed. It is therefore crucial that these parameters are measured or estimated with maximum precision in order to make the most accurate estimation of physiological response, which in turn defines sensation and perception of climate and comfort.

	Climate							
	Moderate				Hot and humid			
Parameter	Value from	Value to	Tcore sensitivity	Tskin sensitivity	Value from	Value to	Tcore sensitivty	Tskin sensitivity
Air temperature, °C	15	28	0.1634	0.3628	22	36	0.4691	0.5703
Mean radiant temperature, °C	22	60	0.0296	0.0110	22	70	0.0840	0.0282
Relative humidity, %	40	80	0.0020	0.0020	50	100	0.1998	0.0280
Wind speed, m/s	0	7	0.2241	0.3026	0	7	0.2906	0.2959
Metabolic rate, W/m2	80	180	0.4361	0.0901	80	180	0.2440	0.0309
Clothing insulation, clo	0.5	1.6	0.1373	0.4924	0.2	1	0.0691	0.3672
Weight, kg	40	120	0.0012	0.0006	40	120	0.0118	0.0006
Height, m	1.5	2	0.0001	0.0001	1.5	2	0.0008	0.0001

FIGURE 2.7: Results of sensitivity analysis for summer seasons in two different climate zones. Colours indicate the sensitivity of the model to a parameter (sensitivity increases from blue to red colour).

2.5 Discussion

In this study, we validated our model against mean skin temperature dynamics as was done by other studies [103, 104]. Multiple studies suggest that this is the most responsive, precisely measurable and representative component of the whole thermophysiological system [120, 121], whereas core temperature is kept by thermoregulatory processes very close to neutral value of around $36.8°C$. So far we demonstrated model performance only in terms of mean skin temperature dynamics in two scenarios found in Munir et al. [103] that consist of stages of neutral, cool and warm environments. In outdoor environments a broader range of parameters is expected and other thermoregulatory aspects become crucial for correct estimation of OTC. For example, in extremely hot environments sweating will play key role in heat dissipation from

the body as well as individual sensation of heat. Calculation of the sweating rate is not a trivial task and no data on sweating rate dynamics has been reported in literature to the best of our knowledge. Sweating rate dynamics can be inferred through evaporation heat loss from the body for which data can be found in the work of Fiala et al. [83]. They report data for an experimental temperature schedule with an extreme hot stage. We simulated this schedule with our new thermoregulatory model and were able to show an excellent correspondence between the simulated and reported data (Figure 2.8). It also demonstrates, that our model is valid for other environments to which it was not particularly calibrated, thus supporting the general validity of the proposed q^*_{bl}.

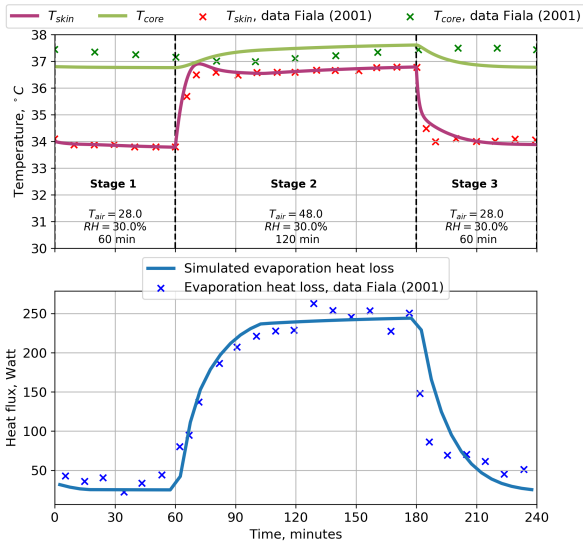

FIGURE 2.8: The performance of the model during the schedule with extremely hot stage (reported in Fiala et al. [83]) demonstrated in skin temperature (top) and evaporation heat loss (bottom) dynamics. Values if evaporation heat loss can considered as direct proxy for sweating rate.

To investigate the performance of the model in cold environments, additional data is required since shivering will play a significant role for thermal sensation and comfort in such cases. Shivering is described by eq. 2.22. Unfortunately this equation has counter intuitive implications if any or both of signals S^-_{core} and S^-_{skin} fall into the range $(-1; 0)$. Alternatively we could use

the shivering description used by Fiala et al. [83]. This however falls outside the scope of this study.

It is worth discussing core-skin blood flow values as they have proven to be crucial for the dynamics of the model. For thermally neutral environments the absolute values of q_{bl}, calculated in the current model (see Figure 2.4b), are 2.8 times larger than those reported in [103, 97, 95] (12.22, 13.49 and 10.6 $l \cdot hr^{-1}$ respectively). A possible explanation for this can be that the first stage in Munir's temperature schedule is not a thermally neutral environment (as is required by the model and its parameters). In fact the core temperature slightly exceeds the level of the core signal T^*_{core} and once this is multiplied by c_{dil}, we see a significant increases in the level of q_{bl}.

The two-node model, which was developed initially for uniform and steady indoor thermal environments, can be applied to dynamic outdoor thermal environments. Even if aspects of the outdoor environment, such as localised direct solar radiation or variable wind flow patterns creating non-uniform heating or cooling of the body, can be taken into account by the currently existing models, then still we are faced with significant experimental uncertainties in obtaining those parameters. The required accurate reproducible measurements needed do not exist at this point in time. This is part of ongoing research in many laboratories.

2.6 Conclusions

Studies of outdoor thermal comfort (OTC) must account for the dynamic nature of the urban microclimate and the physical activity of the subjects. The accuracy of physiological models used for OTC studies should be evaluated not only in equilibrium steady-state conditions, but also in dynamical situations. In this chapter we evaluated and extended the dynamical properties of Gagge's classical model to understand whether the model is appropriate for dynamic assessment of OTC, or whether more sophisticated and computationally expensive models are required.

We provided a detailed specifications of the model parameter values and variable ranges found in literature. A system dynamics representation of the

model, in terms of stocks and flows of energy, gives a highly intuitive understanding of the principles of thermal regulation in the human body and causal relations between climatic, individual and physiological parameters. Implementation of the system dynamics model allows for further exploration of feedback loops and dynamic behaviour of parameters in various scenarios.

Comparing the two-node model with the standard set of parameters and dynamics reported in an empirical study [103] demonstrates discrepancies in the dynamical behaviour of skin temperature. After analysing the model structure, the skin blood flow of the model is identified as the most probable cause of this discrepancy. Optimising the model with parameters of skin blood flow varying within ranges found in literature improves the dynamics. This improvement shows a reduction in RMSE between simulation and empirical data by 17%. The maximum absolute error remains $> 1.3°C$ (Figure 2.4a). Allowing variation in the neutral blood flow results in a new equation for the core-skin blood flow shown in eq. 2.45, RMSE reduction of 73% and the maximum absolute error reduced to $0.63°C$, which is nearly a fourfold improvement in the dynamic behaviour.

$$q_{bl} = \frac{10.7 + 50 \cdot S^{+}_{core}}{1 - 0.1 \cdot S^{-}_{skin}} \qquad \left[\frac{l}{hr \cdot m^2}\right] \tag{2.45}$$

The resulting values of core-skin blood flow are within the standard ranges, this suggests that the modification of neutral skin blood flow is appropriate. Comparing the result of the presented two-node model to results of other multi-node and multi-part models for the same scenario, indicates that highly improved dynamics of skin temperature can be achieved. Due to the unavailability of data the model still requires validation for cold environments.

We have shown that optimised core-skin blood flow allows to accurately reproduce the dynamics, which makes the model amenable for OTC studies, such as: implementation of dynamic Physiologically Equivalent Temperature calculation, investigation of adaptation strategies efficiency and agent-based modelling discussed in Chapter 3, implementation of accumulated heat stress measure used in Chapter 4. The developed system dynamics model can be easily modified to improve, for example, the prediction of individual thermophysiological response, by including parameters of body composition, fitness,

gender and age [122].